RESEARCH ON METHODS OF DYNAMIC MODELING AND SIMULATION FOR MORPHING WING AIRCRAFT

Xu Xiaowu, Zhang Wei
School of Aeronautics, Northwestern Polytechnical University
xuxiaowu19860105@163.com; weizhangxian@nwpu.edu.cn

Keywords: *morphing wing aircraft, dynamics of multi-body systems, modeling, numerical simulation, asymmetric morphing*

Abstract

The purpose of this paper is studying the multi-mode dynamic modeling and dynamic response simulation of a morphing wing aircraft. By using the theory of Dynamics of Multi-body Systems, considering the morphing wing aircraft as full multi-rigid-body systems, the dynamic equations in vector form for every rigid-body are derived. This paper adopts a modular approach to build the nonlinear numerical simulation model, utilizing the Simulink module in the Matlab software. The nonlinear numerical simulation is applied to investigate the characteristics of dynamic response in multi-morphing mode, specifically analyzing the control efficiency of the asymmetry morphing of wing. The results of the numerical simulations show the correctness and feasibility of this method of modeling.

1 Introduction

Morphing wing aircraft are flight vehicles that alter their shape by wing morphing. They can initiatively change the aerodynamic configuration according to the flight environments and combat missions, so as to play the best performance. Aircraft with morphing capability promise the distinct advantage of being able to fly multiple types of missions and to perform extreme maneuvers which is impossible for conventional aircraft designs.

When the morphing process involves large geometrical variations, some characteristics of the aircraft, such as moment of inertia, center of gravity location and focus position, can vary significantly. Consequently, the aerodynamic loads and the flight quality will also be changed, even threatening the flight safety if some kinetic parameters change unexpectedly. Thus it is necessary to analyze the characteristics of dynamic variables of morphing wing aircraft in the morphing process. The investigation shows that the asymmetric sweep is beneficial to maintaining sensor pointing the target despite crosswinds. [1] Morphing wing aircraft can be more propitious to enhance the maneuverability and the agility than conventional aircraft. Thus it is essential to carry out the investigation of the characteristics of aerodynamic loads and dynamic response caused by asymmetric morphing.

In order to study the dynamics and responses of morphing aircraft, many researchers have reformulated the flight dynamics equations of motion assuming the morphing aircraft to be multi-body systems comprising rigid bodies. [2] Seigler *et al* built the dynamic model of large-scale morphing aircraft in theory. [3-5] An *et al* investigated the dynamic response of a variable swept wing aircraft in the process of changing the sweep angle. [6] Yue *et al* modeled and simulated a tailless folding wing morphing aircraft in wing folding process. [7] Niksch *et al* developed an aerodynamic model and a dynamic model of a morphing flying wing aircraft, calculated using a constant strength source doublet panel method. [8-9] Abdulrahim *et al* investigated flight testing, flight performance characteristics, control, and simulation of a multi-role morphing Micro Air Vehicle. [10-12] Grant *et al* introduced a method to relate the flight dynamics of morphing aircraft by interpreting a time-varying eigenvector in terms of flight modes. [13]

However, the investigations in recent years have the following limitations: Many researchers focus on the static analysis of each morphing configuration, the whole aircraft is simplified as a rigid body, and the dynamic response in the morphing procedure cannot be modeled. Utilizing the traditional method based on the separation of longitude and lateral, the dynamic response in some particular morphing procedure cannot be analyzed. These existing methods of modeling cannot be used to analyze dynamic response in the asymmetric morphing process. Consequently, this paper proposes the methods of building dynamic model and numerical simulation of the morphing wing aircraft, which can be used to investigate the dynamic response to the aircraft in the symmetric and asymmetric morphing process.

2 Multi-rigid-body Systems Model

2.1 Model Characterization

Taking one type of folding wing morphing aircraft as an example (see Fig 1), composed of five rigid bodies: the fuselage, two inner wings, and two outer wings. The inner wings can rotate around the axis that is parallel to the fuselage axes. In the process of wing folding, the inner wings rotate and the outer wings keep level.

The morphing wing aircraft is considered as multi-rigid-body systems composed of five rigid bodies hinged in turn. These bodies are noted in rule method [14]. B_1 is the fuselage, B_2 and B_4 are the inner wings, B_3 and B_5 are the outer wings. C_i (i=1, 2, 3, 4, 5) is the center of gravity of B_i. The aircraft's center of gravity at the configuration of wing unfold is selected as the virtual hinge O_1 which is fixed to the inertial coordinate. The five rigid bodies are connected to a multiple rigid body system by other four cylindrical hinges O_i (i=2, 3, 4, 5). The virtual hinge O_1 contains three rotational DOF and three translational DOF, while other hinges have one rotational DOF. For this configuration the shape variation depends on θ_1 and θ_2, the right and left folding angles respectively. $\boldsymbol{d}_{ij}$ is named as access vector, which is defined in the Reference [14].

It is possible to define a local coordinate system S_i-$O_ix_iy_iz_i$ for the i-th body (see Fig 1). The local coordinate system of B_1 is the same as the body coordinate system, of which the origin is located at the aircraft's center of gravity at the configuration of wing unfold.

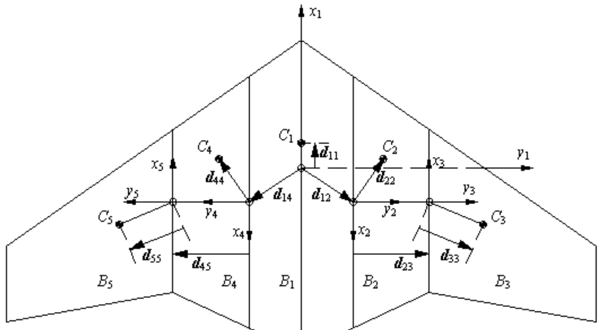

(a) Wing unfold (planform)

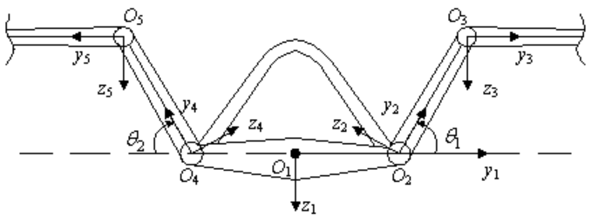

(b) Wing folding process (rearview)

Fig 1. Multi-rigid-body Systems Model of folding wing morphing aircraft

2.2 Kinematic analysis

An orthonormal transformation between the axes S_1 and S_i is performed through $\boldsymbol{A}_{1i}$. The access vector $\boldsymbol{d}_{ij}$ in the local coordinate system of i-th body can be expressed as

$$\boldsymbol{d}_{ij}^{(i)}=(d_{ijx} \quad d_{ijy} \quad d_{ijz})^{\mathrm{T}} \tag{1}$$

Access vector $\boldsymbol{d}_{ij}$ in the body coordinate system can be obtained as

$$\boldsymbol{d}_{ij}^{(1)}=\boldsymbol{A}_{1i}\boldsymbol{d}_{ij}^{(i)} \tag{2}$$

Consider a velocity vector $\boldsymbol{V}$ and an angular velocity vector $\boldsymbol{\Omega}$ expressed in the body coordinate system of the morphing wing aircraft.

$$\boldsymbol{V}=(u \quad v \quad w)^{\mathrm{T}} \tag{3}$$

$$\boldsymbol{\Omega}=(p \quad q \quad r)^{\mathrm{T}} \tag{4}$$

Assuming the fold angular velocity is constant, the right rotation rate and the left rotation rate in the body coordinate system can be respectively expressed as

$$\boldsymbol{\omega}_1 = (-\dot{\theta}_1 \quad 0 \quad 0)^{\mathrm{T}} \tag{5}$$

$$\boldsymbol{\omega}_2 = (\dot{\theta}_2 \quad 0 \quad 0)^{\mathrm{T}} \tag{6}$$

Then it is easy to obtain the velocity vector $\boldsymbol{V}_i$, the angular velocity vector $\boldsymbol{\Omega}_i$, and the angular velocity acceleration vector $\dot{\boldsymbol{\Omega}}_i$ of i-th (i=2, 3, 4, 5) body, which are expressed in the body coordinate system of the morphing wing aircraft.

$$\begin{aligned}
&\boldsymbol{V}_2 = \boldsymbol{V} + \boldsymbol{\omega}_1 \times \boldsymbol{d}_{22}^{(1)}; \boldsymbol{\Omega}_2 = \boldsymbol{\Omega} + \boldsymbol{\omega}_1; \\
&\qquad \dot{\boldsymbol{\Omega}}_2 = \dot{\boldsymbol{\Omega}} + \dot{\boldsymbol{\Omega}} \times \boldsymbol{\omega}_1 \\
&\boldsymbol{V}_3 = \boldsymbol{V} + \boldsymbol{\omega}_1 \times \boldsymbol{d}_{23}^{(1)}; \boldsymbol{\Omega}_3 = \boldsymbol{\Omega}; \dot{\boldsymbol{\Omega}}_3 = \dot{\boldsymbol{\Omega}} \\
&\boldsymbol{V}_4 = \boldsymbol{V} + \boldsymbol{\omega}_2 \times \boldsymbol{d}_{44}^{(1)}; \boldsymbol{\Omega}_4 = \boldsymbol{\Omega} + \boldsymbol{\omega}_2; \\
&\qquad \dot{\boldsymbol{\Omega}}_4 = \dot{\boldsymbol{\Omega}} + \dot{\boldsymbol{\Omega}} \times \boldsymbol{\omega}_2 \\
&\boldsymbol{V}_5 = \boldsymbol{V} + \boldsymbol{\omega}_2 \times \boldsymbol{d}_{45}^{(1)}; \boldsymbol{\Omega}_5 = \boldsymbol{\Omega}; \dot{\boldsymbol{\Omega}}_5 = \dot{\boldsymbol{\Omega}}
\end{aligned} \tag{7}$$

3 Equations of Motion

3.1 Dynamic Equations

The dynamics equations of each rigid are obtained from Newton's second law. Newton's second law can be expressed by the vectors defined in Equations (8) and (9).

Force equation:

$$\frac{1}{m_i}(\sum \boldsymbol{F}_i)_B = \left(\frac{d\boldsymbol{V}_i}{dt}\right)_B^B + (\boldsymbol{\Omega}_i)_B^I \times (\boldsymbol{V}_i)_B \tag{8}$$

Moment equation:

$$(\sum \boldsymbol{M}_i)_B = \left(\frac{d\boldsymbol{H}_i}{dt}\right)_B^B + (\boldsymbol{\Omega}_i)_B^I \times (\boldsymbol{H}_i)_B \tag{9}$$

Where i=1, 2, 3, 4, 5. The superscript I indicates the derivative of the vector in the inertial coordinate, and the subscript B indicates the component in the body coordinate. $\boldsymbol{F}_i$ is the summation of the outside forces applied to the i-th rigid body, and the outside forces include gravity, aerodynamic load, constrained force between each rigid body, and thrust of the engine (for the rigid body with engine). $\boldsymbol{M}_i$ is the summation of the outside moments applied to the i-th rigid body, and the outside moments are caused by the gravity, aerodynamic load, constrained moment between each rigid body, and thrust of the engine (for the rigid body with engine). m_i is the mass of i-th rigid body. $\boldsymbol{V}_i$, $\boldsymbol{\Omega}_i$ and $\boldsymbol{H}_i$ ($\boldsymbol{H}_i = \boldsymbol{I}_i\boldsymbol{\Omega}_i$) indicate the component of velocity, angle velocity and momentum moment in the body coordinate, respectively. $\boldsymbol{I}_i$ is the inertia tensor of i-th rigid body expressed in the body coordinate, which is defined as

$$\boldsymbol{I}_i = \begin{bmatrix} I_{ixx} & -I_{ixy} & -I_{ixz} \\ -I_{ixy} & I_{iyy} & -I_{iyz} \\ -I_{ixz} & -I_{iyz} & I_{izz} \end{bmatrix} \tag{10}$$

By applying equations (3)~(4), and (7)~(9), the dynamic equations to the i-th rigid body can be expressed in the following vector form:

$$\begin{aligned}
&\sum \boldsymbol{F}_1 = m_1[\dot{\boldsymbol{V}} + \boldsymbol{\Omega} \times \boldsymbol{V}] \\
&\sum \boldsymbol{F}_2 = m_2[\dot{\boldsymbol{V}} + \boldsymbol{\omega}_1 \times (\boldsymbol{\omega}_1 \times \boldsymbol{d}_{22}^{(1)}) + \\
&\qquad (\boldsymbol{\Omega} + \boldsymbol{\omega}_1) \times (\boldsymbol{V} + \boldsymbol{\omega}_1 \times \boldsymbol{d}_{22}^{(1)})] \\
&\sum \boldsymbol{F}_3 = m_3[\dot{\boldsymbol{V}} + \boldsymbol{\omega}_1 \times (\boldsymbol{\omega}_1 \times \boldsymbol{d}_{23}^{(1)}) + \\
&\qquad \boldsymbol{\Omega} \times (\boldsymbol{V} + \boldsymbol{\omega}_1 \times \boldsymbol{d}_{23}^{(1)})] \\
&\sum \boldsymbol{F}_4 = m_4[\dot{\boldsymbol{V}} + \boldsymbol{\omega}_2 \times (\boldsymbol{\omega}_2 \times \boldsymbol{d}_{44}^{(1)}) + \\
&\qquad (\boldsymbol{\Omega} + \boldsymbol{\omega}_2) \times (\boldsymbol{V} + \boldsymbol{\omega}_2 \times \boldsymbol{d}_{44}^{(1)})] \\
&\sum \boldsymbol{F}_5 = m_5[\dot{\boldsymbol{V}} + \boldsymbol{\omega}_2 \times (\boldsymbol{\omega}_2 \times \boldsymbol{d}_{45}^{(1)}) + \\
&\qquad \boldsymbol{\Omega} \times (\boldsymbol{V} + \boldsymbol{\omega}_2 \times \boldsymbol{d}_{45}^{(1)})]
\end{aligned} \tag{11}$$

$$\begin{aligned}
&\sum \boldsymbol{M}_1 = \boldsymbol{I}_1\dot{\boldsymbol{\Omega}} + \boldsymbol{\Omega} \times (\boldsymbol{I}_1\boldsymbol{\Omega}) \\
&\sum \boldsymbol{M}_2 = \dot{\boldsymbol{I}}_2(\boldsymbol{\Omega} + \boldsymbol{\omega}_1) + \boldsymbol{I}_2(\dot{\boldsymbol{\Omega}} + \boldsymbol{\Omega} \times \boldsymbol{\omega}_1) \\
&\qquad + (\boldsymbol{\Omega} + \boldsymbol{\omega}_1) \times [\boldsymbol{I}_2(\boldsymbol{\Omega} + \boldsymbol{\omega}_1)] \\
&\sum \boldsymbol{M}_3 = \dot{\boldsymbol{I}}_3\boldsymbol{\Omega} + \boldsymbol{I}_3\dot{\boldsymbol{\Omega}} + \boldsymbol{\Omega} \times (\boldsymbol{I}_3\boldsymbol{\Omega}) \\
&\sum \boldsymbol{M}_4 = \dot{\boldsymbol{I}}_4(\boldsymbol{\Omega} + \boldsymbol{\omega}_2) + \boldsymbol{I}_4(\dot{\boldsymbol{\Omega}} + \boldsymbol{\Omega} \times \boldsymbol{\omega}_2) \\
&\qquad + (\boldsymbol{\Omega} + \boldsymbol{\omega}_2) \times [\boldsymbol{I}_4(\boldsymbol{\Omega} + \boldsymbol{\omega}_2)] \\
&\sum \boldsymbol{M}_5 = \dot{\boldsymbol{I}}_5\boldsymbol{\Omega} + \boldsymbol{I}_5\dot{\boldsymbol{\Omega}} + \boldsymbol{\Omega} \times (\boldsymbol{I}_5\boldsymbol{\Omega})
\end{aligned} \tag{12}$$

The constrained forces and moments between each rigid body are counteracted, and then only gravity, aerodynamic load, and thrust of the engine are left on the left of the dynamic equations. In the body coordinate system, the total forces and moments can be expressed as

$$\boldsymbol{F}_B = (F_x \quad F_y \quad F_z)^{\mathrm{T}} \tag{13}$$

$$\boldsymbol{M}_B = (L \quad M \quad N)^{\mathrm{T}} \tag{14}$$

The dynamic equations can be collected and expressed in the form of component set, as shown in Equations (15) and (16).

$$\begin{aligned}
&F_x = m(\dot{u} + qw - rv) - m_2 d_{22y}\dot{\theta}_1(q\cos\theta_1 - r\sin\theta_1) \\
&-m_3 d_{23y}\dot{\theta}_1(q\cos\theta_1 - r\sin\theta_1) - m_4 d_{44y}\dot{\theta}_2(q\cos\theta_2 \\
&+r\sin\theta_2) - m_5 d_{45y}\dot{\theta}_2(q\cos\theta_2 + r\sin\theta_2) \\
&F_y = m(\dot{v} + ru - pw) + m_2[w\dot{\theta}_1 + d_{22y}\dot{\theta}_1(p - 2\dot{\theta}_1) \\
&\cos\theta_1] + m_3 d_{23y}\dot{\theta}_1(p - \dot{\theta}_1)\cos\theta_1 + m_4[-w\dot{\theta}_2 + \\
&d_{44y}\dot{\theta}_2(p + 2\dot{\theta}_2)\cos\theta_2] + m_5 d_{45y}\dot{\theta}_2(p + \dot{\theta}_2)\cos\theta_2 \\
&F_z = m(\dot{w} + pv - qu) - m_2[v\dot{\theta}_1 + d_{22y}\dot{\theta}_1(p - 2\dot{\theta}_1) \\
&\sin\theta_1] - m_3 d_{23y}\dot{\theta}_1(p - \dot{\theta}_1)\sin\theta_1 + m_4[v\dot{\theta}_2 + d_{44y}\dot{\theta}_2 \\
&(p + 2\dot{\theta}_2)\sin\theta_2] + m_5 d_{45y}\dot{\theta}_2(p + \dot{\theta}_2)\sin\theta_2
\end{aligned} \tag{15}$$

$$\begin{aligned}
&L = \dot{p}I_{xx} + qr(I_{zz} - I_{yy}) + (pr - \dot{q})I_{xy} - (\dot{r} + pq)I_{xz} \\
&+(r^2 - q^2)I_{yz} + (p - \dot{\theta}_1)\dot{I}_{2xx} - q\dot{I}_{2xy} - r\dot{I}_{2xz} + p\dot{I}_{3xx} \\
&-q\dot{I}_{3xy} - r\dot{I}_{3xz} + (p + \dot{\theta}_2)\dot{I}_{4xx} - q\dot{I}_{4xy} - r\dot{I}_{4xz} + p\dot{I}_{5xx} \\
&-q\dot{I}_{5xy} - r\dot{I}_{5xz} \\
&M = \dot{q}I_{yy} + pr(I_{xx} - I_{zz}) - (qr + \dot{p})I_{xy} + (p^2 - r^2)I_{xz} \\
&+(pq - \dot{r})I_{yz} + r\dot{\theta}_1(I_{2zz} - I_{2xx} - I_{2yy}) + (\dot{\theta}_1 - 2p\dot{\theta}_1) \\
&I_{2xz} - 2q\dot{\theta}_1 I_{2yz} + q\dot{I}_{2yy} - (p - \dot{\theta}_1)\dot{I}_{2xy} - r\dot{I}_{2yz} + q\dot{I}_{3yy} \\
&-p\dot{I}_{3xy} - r\dot{I}_{3yz} + r\dot{\theta}_2(I_{4xx} + I_{4yy} - I_{4zz}) + (\dot{\theta}_2 + 2p\dot{\theta}_2) \\
&I_{4xz} + 2q\dot{\theta}_2 I_{4yz} + q\dot{I}_{4yy} - (p + \dot{\theta}_2)\dot{I}_{4xy} - r\dot{I}_{4yz} + q\dot{I}_{5yy} \\
&-p\dot{I}_{5xy} - r\dot{I}_{5yz} \\
&N = \dot{r}I_{zz} + pq(I_{yy} - I_{xx}) + (q^2 - p^2)I_{xy} + (qr - \dot{p})I_{xz} \\
&-(pr + \dot{q})I_{yz} + q\dot{\theta}_1(I_{2xx} + I_{2zz} - I_{2yy}) - (\dot{\theta}_1 - 2p\dot{\theta}_1) \\
&I_{2xy} - 2r\dot{\theta}_1 I_{2yz} + r\dot{I}_{2zz} - (p - \dot{\theta}_1)\dot{I}_{2xz} - q\dot{I}_{2yz} + r\dot{I}_{3zz} - \\
&p\dot{I}_{3xz} - q\dot{I}_{3yz} + q\dot{\theta}_2(I_{4yy} - I_{4xx} - I_{4zz}) - (\dot{\theta}_2 + 2p\dot{\theta}_2) \\
&I_{4xy} - 2r\dot{\theta}_2 I_{4yz} + r\dot{I}_{4zz} - (p + \dot{\theta}_2)\dot{I}_{4xz} - q\dot{I}_{4yz} + r\dot{I}_{5zz} \\
&-p\dot{I}_{5xz} - q\dot{I}_{5yz}
\end{aligned} \tag{16}$$

Where m is the mass of the morphing wing aircraft. $I_{xx}, I_{yy}, I_{zz}, I_{xy}, I_{xz}$ and I_{yz} are the sum of inertia items of rigid bodies.

3.2 Kinematics Equations

By transforming the Euler angles into the body coordinate system, three nonlinear body rate equations can be written, as seen in Equation (17).

$$\begin{aligned}
&p = \dot{\phi} - \dot{\psi}\sin\theta \\
&q = \dot{\theta}\cos\phi + \dot{\psi}\cos\theta\sin\phi \\
&r = -\dot{\theta}\sin\phi + \dot{\psi}\cos\theta\cos\phi
\end{aligned} \tag{17}$$

An Euler transformation may be used to transform the body velocities into the desired Earth-defined velocities, as seen in Equation (18).

$$\begin{aligned}
\dot{x}_g &= u\cos\theta\cos\psi + v(\sin\theta\cos\psi\sin\phi - \sin\psi \\
&\quad \cos\phi) + w(\sin\theta\cos\psi\cos\phi + \sin\psi\sin\phi) \\
\dot{y}_g &= u\cos\theta\sin\psi + v(\sin\theta\sin\psi\sin\phi + \cos\psi \\
&\quad \cos\phi) + w(\sin\theta\sin\psi\sin\phi - \cos\psi\sin\phi) \\
\dot{h} &= u\sin\theta - v\cos\theta\sin\phi - w\cos\theta\cos\phi
\end{aligned} \tag{18}$$

Equations (15) ~ (18) are the same as the six-DOF nonlinear equations of conventional configuration aircraft.

3.3 Aerodynamic Force and Moment

References [6] and [7] have shown that when the morphing rate is not very big, the dynamic response affected by unsteady aerodynamic force caused by morphing can be ignored. Thus in this paper the unsteady aerodynamic effect is not considered and the aerodynamic force and moment are gained by quasi-steady assumption that the aerodynamic force of the morphing wing aircraft under certain configuration in morphing process nearly equals to that of corresponding static configuration. Then the forces and moments of the morphing wing aircraft in morphing process can be expressed as

$$\begin{aligned}
&F_{A,x} = qS_w(C_L\sin\alpha - C_D\cos\alpha) \\
&F_{A,y} = qS_w C_Y + F_{u,y} \\
&F_{A,z} = qS_w(-C_D\sin\alpha - C_L\cos\alpha) \\
&L_A = qS_w b_w(C_l\cos\alpha - C_n\sin\alpha) + L_u \\
&M_A = qS_w c_A C_m \\
&N_A = qS_w b_w(C_n\cos\alpha + C_l\sin\alpha) + N_u
\end{aligned} \tag{19}$$

Where $F_{u,y}$, L_u and N_u, i.e. side-force, rolling moment and yaw moment caused by the shape variation, which depends on θ_1 and θ_2.

In order to describe $F_{u,y}$, L_u and N_u, Note the radius vectors from the origin of body coordinate to the aerodynamic center of i-th (i=2, 3, 4, 5) rigid body as $\boldsymbol{r}_{ci}$,which can be expressed as

$$\boldsymbol{r}_{ci} = (r_{cix} \quad r_{ciy} \quad r_{ciz})^{\mathrm{T}} \tag{20}$$

Note the vectors from the hinge of i-th (i=2, 3, 4, 5) rigid body to the aerodynamic center of i-th rigid body as $\boldsymbol{a}_{ii}$. In the local coordinate it can be expressed as

$$\boldsymbol{a}_{ii}^{(i)} = (\boldsymbol{a}_{iix} \quad \boldsymbol{a}_{iiy} \quad \boldsymbol{a}_{iiz})^{\mathrm{T}} \tag{21}$$

According to the orthonormal transformation between axes S_1 and S_i, $\boldsymbol{a}_{ii}$ can be expressed in the body coordinate as

$$\boldsymbol{a}_{ii}^{(1)} = \boldsymbol{A}_{1i}\boldsymbol{a}_{ii}^{(i)} \tag{22}$$

Then it is easy to obtain $\boldsymbol{r}_{ci}$, expressed as

$$\begin{aligned}
\boldsymbol{r}_{c2} &= \boldsymbol{d}_{12} + \boldsymbol{A}_{12}\boldsymbol{a}_{22}^{(2)} \\
\boldsymbol{r}_{c3} &= \boldsymbol{d}_{12} + \boldsymbol{A}_{12}\boldsymbol{d}_{23}^{(2)} + \boldsymbol{A}_{13}\boldsymbol{a}_{33}^{(3)} \\
\boldsymbol{r}_{c4} &= \boldsymbol{d}_{14} + \boldsymbol{A}_{14}\boldsymbol{a}_{44}^{(4)} \\
\boldsymbol{r}_{c5} &= \boldsymbol{d}_{14} + \boldsymbol{A}_{14}\boldsymbol{d}_{45}^{(4)} + \boldsymbol{A}_{15}\boldsymbol{a}_{55}^{(5)}
\end{aligned} \tag{23}$$

Finally, the expression of $F_{u,y}$, L_u and N_u can be obtained as

$$F_{u,y} = (\sin\theta_2 - \sin\theta_1)\cdot C_L \cdot \cos\alpha \cdot q \cdot S_2 \tag{24}$$

$$\begin{aligned}
L_u = (&r_{c2z}\cdot\sin\theta_1 - r_{c2y}\cdot\cos\theta_1 - r_{c4y}\cdot\cos\theta_2 \\
&- r_{c4z}\cdot\sin\theta_2)\cdot C_L\cdot\cos\alpha\cdot q\cdot S_2 - (r_{c3y} \\
&+ r_{c5y})\cdot C_L\cdot\cos\alpha\cdot q\cdot S_3
\end{aligned} \tag{25}$$

$$N_u = (\sin\theta_2 - \sin\theta_1)\cdot r_{c2x}\cdot C_L\cdot\cos\alpha\cdot q\cdot S_2 \tag{26}$$

Where S_2 is the inner wing reference area, S_3 is the outer wing reference area.

4 Morphing Wing Aircraft Model

4.1 Geometry configurations

Taking a micro folding wing morphing aircraft as an example, it has flying wing configuration and consists of an inlet on the back of fuselage, a W-type tail skirt and a beavertail on the tailing (see Fig 2). Two separate actuators allow the inner wings to rotate related to the axes which are parallel to the fuselage axis, modifying the dihedral angles up to 120° while the outer wings keep level. Longitudinal and lateral controls are provided by a pair of elevons arranged on the outer wings. The pair of elevons has deflection range of -20°~30°. The main parameters of wing fold and unfold are listed in Table 1.

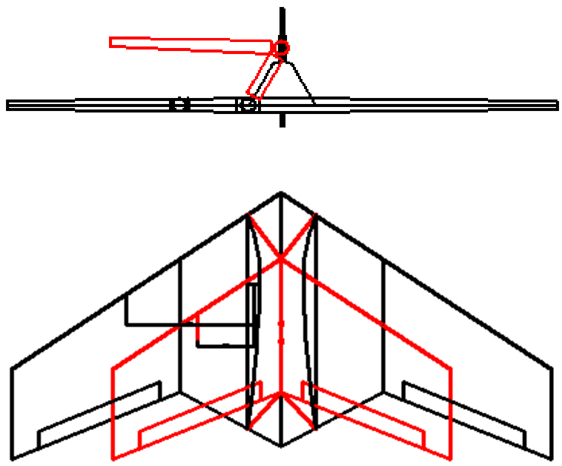

Fig 2. Planform and rearview of folding wing morphing aircraft

Table 1. Parameters of wing fold and unfold

Parameters	wing fold	wing unfold
Wing Span (m)	2.0	1.1
Wing Area (m^2)	0.81	0.55
Loading (kg/m^2)	4.82	7.10
Sweep Angle (°)	30	30
Aspect Ratio	4.9	2.2
Taper Ratio	0.24	0.30
Weight (kg)	3.9	
Length (m)	0.9	
Thrust Loading	0.78	

The main geometrical parameters of bodies are listed in Table 2.

Table 2. Parameters of bodies

Parameters	Fuselage	Inner Wing	Outer Wing
Span (m)	0.30	0.30	0.55
Area (m^2)	0.218	0.131	0.165

Root Chord (m)	0.900	0.725	0.468
Tip Chord (m)	0.725	0.468	0.217
Sweep Angle (°)	35	35	35

4.2 Mass and Inertia Properties

As depicted in Fig 3, the multi-rigid body is approximated to a system composed of a single fuselage and four point masses each capable of motion relative to the main body. [4] The mass and inertia properties of fuselage, inner wing, and outer wing are presented in Table 3.

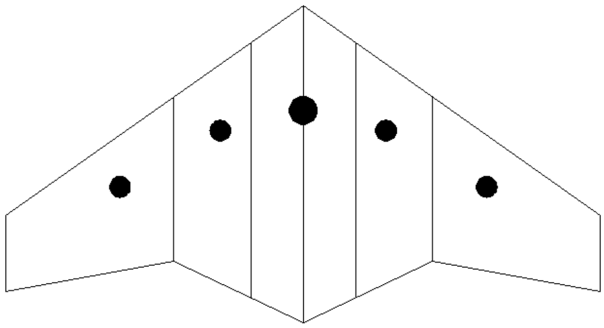

Fig 3. Depiction of the Multi-Mass Approximation

Table 3. Mass and Inertia properties

Parameters	Fuselage	Inner Wing	Outer Wing
Mass (kg)	2.14	0.52	0.36
I_{xx} (kg*m^2)	0.015	0.0011	0.007
I_{yy} (kg*m^2)	0.068	0.008	0.005
I_{zz} (kg*m^2)	0.078	0.008	0.01
I_{xy} (kg*m^2)	0	0.0005	0.005
I_{xz} (kg*m^2)	0.002	0	0
I_{yz} (kg*m^2)	0	0	0

For this configuration the center of gravity location and the inertia tensor are functions of θ_1 and θ_2. They can be expressed as

$$\mathbf{x}_{cg} = \mathbf{x}_{cg}(\theta_1, \theta_2) \tag{27}$$

$$\boldsymbol{I} = \boldsymbol{I}(\theta_1, \theta_2) \tag{28}$$

The inertia tensor $\boldsymbol{I}_i$ of the i-th body with respect to the body coordinate can be expressed as

$$\boldsymbol{I}_i = \boldsymbol{A}_{1i}\boldsymbol{I}_{ci}\boldsymbol{A}_{1i}^{\mathrm{T}} + m_i(\boldsymbol{\rho}_{ci}^{\mathrm{T}}\boldsymbol{\rho}_{ci}\mathbf{E} - \boldsymbol{\rho}_{ci}\boldsymbol{\rho}_{ci}^{\mathrm{T}}) \tag{29}$$

Where $\boldsymbol{I}_{ci}$ is the inertia tensor of the i-th body with respect to the local coordinate. $\mathbf{E}$ is the identity matrix of 3×3. $\boldsymbol{\rho}_{ci}$ is the radius vectors from the origin of body coordinate to the i-th body's center of gravity, expressed as

$$\boldsymbol{\rho}_{ci} = (\rho_{cix} \quad \rho_{ciy} \quad \rho_{ciz})^{\mathrm{T}} \tag{30}$$

The $\boldsymbol{\rho}_{ci}$ can be calculated as

$$\begin{aligned} \boldsymbol{\rho}_{c1} &= \boldsymbol{d}_{11} \\ \boldsymbol{\rho}_{c2} &= \boldsymbol{d}_{12} + \boldsymbol{A}_{12}\boldsymbol{d}_{22}^{(2)} \\ \boldsymbol{\rho}_{c3} &= \boldsymbol{d}_{12} + \boldsymbol{A}_{12}\boldsymbol{d}_{23}^{(2)} + \boldsymbol{A}_{13}\boldsymbol{d}_{33}^{(3)} \\ \boldsymbol{\rho}_{c4} &= \boldsymbol{d}_{14} + \boldsymbol{A}_{14}\boldsymbol{d}_{44}^{(4)} \\ \boldsymbol{\rho}_{c5} &= \boldsymbol{d}_{14} + \boldsymbol{A}_{14}\boldsymbol{d}_{45}^{(4)} + \boldsymbol{A}_{15}\boldsymbol{d}_{55}^{(5)} \end{aligned} \tag{31}$$

Taking the time derivative of the Equation (29), the rate of inertia tensor is obtained, note as $\dot{\boldsymbol{I}}_i$

$$\begin{aligned} \dot{\boldsymbol{I}}_i = {} & \dot{\boldsymbol{A}}_{1i}\boldsymbol{I}_{ci}\boldsymbol{A}_{1i}^{\mathrm{T}} + \boldsymbol{A}_{1i}\boldsymbol{I}_{ci}\dot{\boldsymbol{A}}_{1i}^{\mathrm{T}} + m_i[(\dot{\boldsymbol{\rho}}_{ci}^{\mathrm{T}}\boldsymbol{\rho}_{ci} \\ & + \boldsymbol{\rho}_{ci}^{\mathrm{T}}\dot{\boldsymbol{\rho}}_{ci})\mathbf{E} - (\dot{\boldsymbol{\rho}}_{ci}\boldsymbol{\rho}_{ci}^{\mathrm{T}} + \boldsymbol{\rho}_{ci}\dot{\boldsymbol{\rho}}_{ci}^{\mathrm{T}})] \end{aligned} \tag{32}$$

Finally, the global inertia tensor and the rate of global inertia tensor can be calculated as

$$\boldsymbol{I} = \sum_{i=1}^{5} \boldsymbol{I}_i \tag{33}$$

$$\dot{\boldsymbol{I}} = \sum_{i=1}^{5} \dot{\boldsymbol{I}}_i \tag{34}$$

Figs 4 and 5 show the variation of the inertia and rate of inertia when the inner wings fold symmetrically and asymmetrically. It can be seen that some inertia coupling items (I_{xy}, I_{yz}, $\dot{I}_{xy}$ and $\dot{I}_{yz}$) arise when the inner wings are folded asymmetrically.

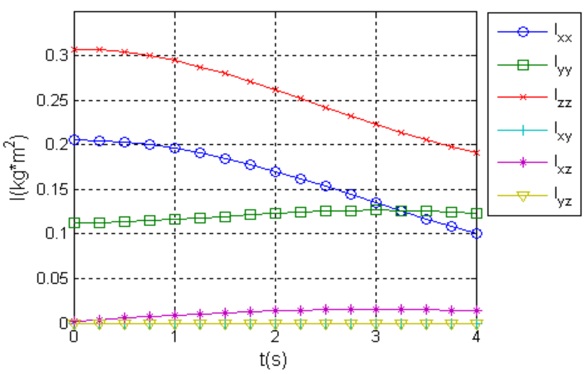

(a) Inertia

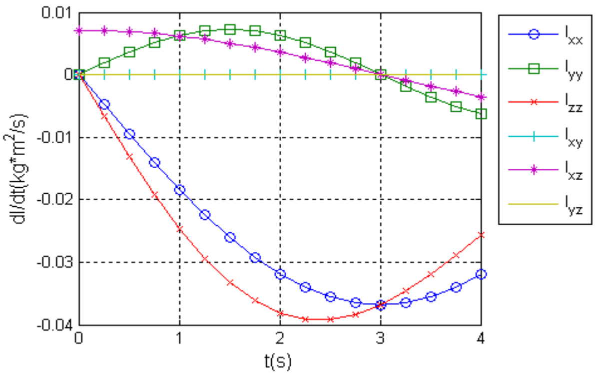

(b) Inertia first order time derivative
Fig 4. Inertia and rate of inertia variation when both inner wings are folded from 0 to 120 deg

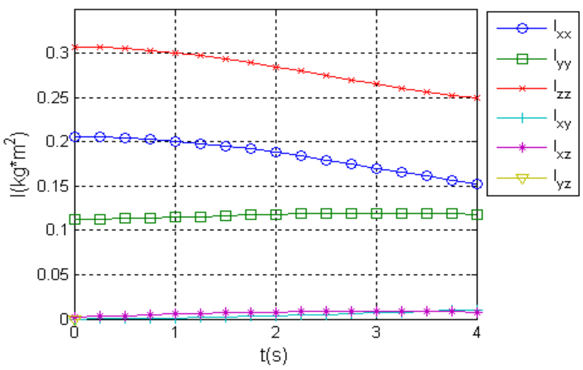

(a) Inertia

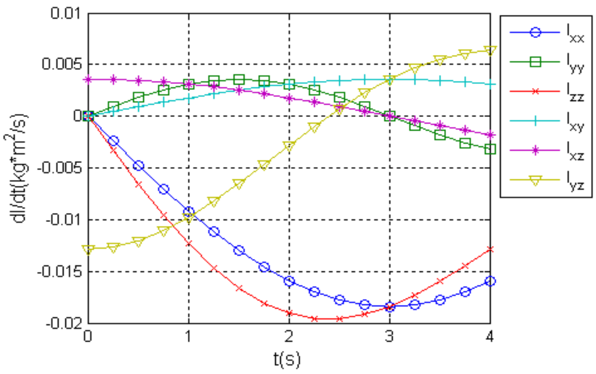

(b) Inertia first order time derivative
Fig 5. Inertia and rate of inertia variation when right inner wing is folded from 0 to 120 deg

5 Dynamic Simulation

5.1 Simulation Model

Based on the dynamic model, the nonlinear numerical simulation model is built utilizing the Simulink module in the Matlab software. Using a modular approach to build the simulation model composed of five model blocks. The block diagrams are shown in the Figs 6 to 10.

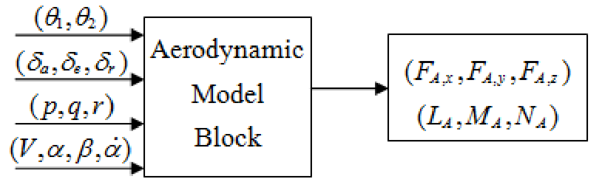

Fig 6. Aerodynamic model block input-output scheme

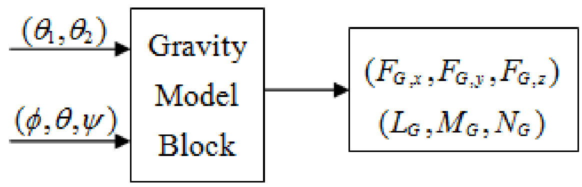

Fig 7. Gravity model block input-output scheme

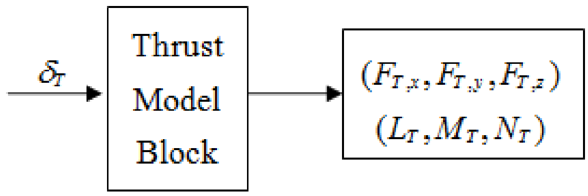

Fig 8. Thrust model block input-output scheme

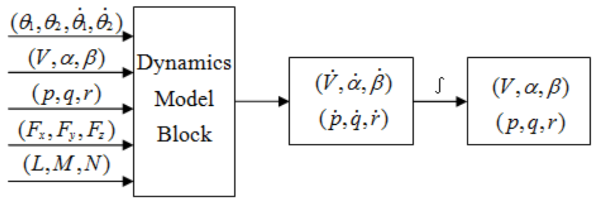

Fig 9. Dynamics model block input-output scheme

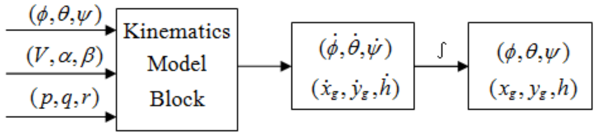

Fig 10. Kinematics model block input-output scheme

5.2 Numerical simulation

The dynamic response of symmetrical folding and asymmetrical folding is simulated respectively (see Figs 11 and 12) in a steady longitudinal condition of flight in which the equilibrium states and controls are the following:

$$
\begin{aligned}
&h = 500m, V = 20m/s \\
&a, \theta = 3.0°, \delta_e = -1.4° \\
&p, q, r, \beta, \phi, \psi = 0 \qquad\qquad (35) \\
&\delta_a, \delta_r, \theta_1, \theta_1 = 0 \\
&\delta_T = 0.187[0-1]
\end{aligned}
$$

Both the symmetrical folding ($\dot{\theta}_1 = \dot{\theta}_2 = 30°/s$) and the asymmetrical folding ($\dot{\theta}_1 = 30°/s, \dot{\theta}_2 = 0$) are completed in 4 seconds, no controls in the folding process.

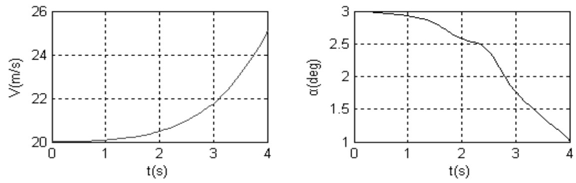

(a) (b)

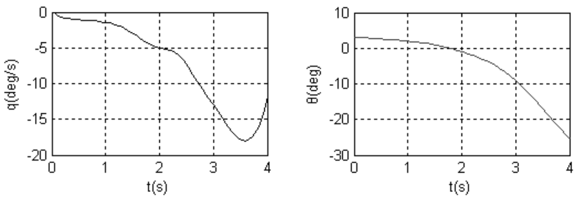

(c) (d)

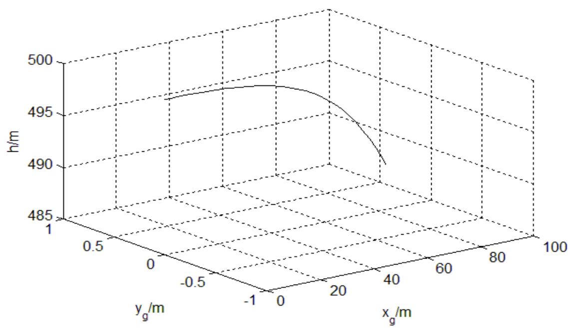

(e)

Fig 11. Dynamic response of symmetrical folding

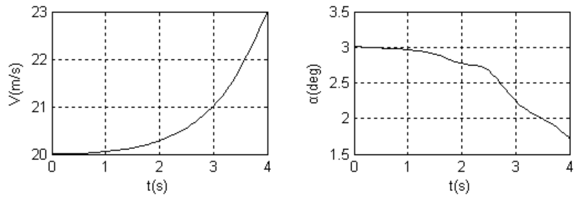

(a) (b)

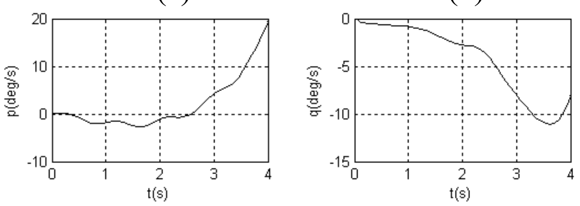

(c) (d)

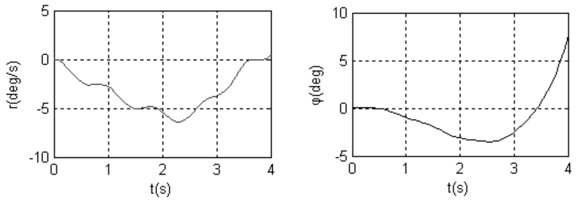

(e) (f)

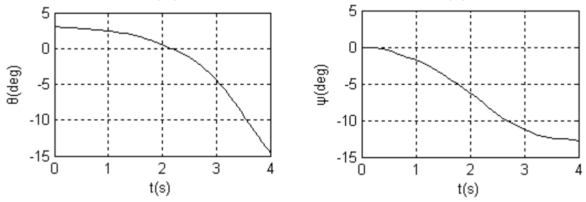

(g) (h)

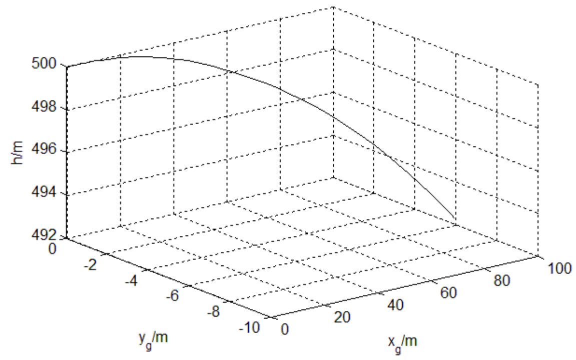

(i)

Fig 12. Dynamic response of asymmetrical folding

As seen in Fig 11, when the wings begin to symmetrically fold, the dynamic response mainly represents the variation of angle of attack, pitch angular velocity and pitch angle. Yet because of the pitch-damping, these variations are limited. As the aerodynamic center of aircraft continues to shift back in wing folding, which will produce a nose-down pitching moment, and then these variations increase sharply.

Fig 12 shows that when the wings begin to asymmetrically fold, the longitudinal dynamic response is similar to the symmetrical process, but the variations are smaller than the symmetrical process. When the right wings begin to fold, the influence of inertia moment is larger than the aerodynamic force and moment change, so the aircraft rolls to the left. Afterwards, the aerodynamic force and moment will largely affect the dynamic response, so the aircraft will stop rolling left and roll to the right.

5 Conclusion

This paper presents a new method of dynamic modeling with the theories of Dynamics of Multi-body Systems. Considering the folding wing morphing aircraft as a full multi-rigid-body system, the dynamic equations that can depict the whole morphing process are derived. Then this paper investigates the mass and inertia properties during the aircraft morphing. Considering the effect of the morphing control input on the aerodynamic force, the expressions of the force and moment are derived. The characteristics of dynamic variables are investigated during the symmetry and asymmetry morphing. Based on this model, the nonlinear numerical simulation model is built utilizing the Simulink module in the Matlab software, and then implements the simulation by taking a folding wing morphing aircraft as an example. The results of the numerical simulations show the correctness of this method of modeling.

References

[1] Grant D T. *Modeling and Dynamic analysis of a multi-joint Morphing aircraft*. Master' degree, University of Florida, 2009.
[2] Ameri N, Lowenberg M H and Friswell M I. Modeling the Dynamic Response of a Morphing Wing with Active Winglets. *AIAA Atmospheric Flight Mechanics Conference and Exhibit*, Hilton Head, South Carolina, AIAA Paper 2007-6500, 20-23 August 2007.
[3] Seigler T M, Neal D A and Inman D J. Dynamic Modeling of Large-Scale Morphing Aircraft. *47th AIAA/ASME/ASCE/AHS/ASC Structures, Structural Dynamics & Materials Conference*, Newport, Rhode Island, AIAA Paper 2006-1893, 1-4 May 2006.
[4] Seigler T M. *Dynamics and Control of Morphing Aircraft*. Doctor' degree, Virginia Polytechnic Institute and State University, 2005.
[5] Seigler T M and Neal D A. Modeling and flight control of Large-Scale Morphing Aircraft. *Journal of Aircraft*, Vol. 44, No. 4, pp 1077-1087, 2007.
[6] An J G, Yan M and Zhou W B. Aircraft Dynamic Response to Variable Wing Sweep Geometr. *Journal of Aircraft*, Vol. 25, No. 3, pp 216-221, 1988.
[7] Yue T, Wang L X and Ai J Q. Multibody Dynamic Modeling and Simulation of a Tailless Folding Wing Morphing Aircraft. *AIAA Atmospheric Flight Mechanics Conference*, Chicago, Illinois, AIAA Paper 2009-6155, 10-13 August 2009.
[8] Niksch A, Valasek J, Strganac T W and Carlson L A. Morphing Aircraft Dynamical Model: Longitudinal Shape Changes. *AIAA Atmospheric Flight Mechanics Conference and Exhibit*, Honolulu, Hawaii, AIAA Paper 2008-6567, 18-21 August, 2008.
[9] Niksch A, Valasek J, Strganac T W and Carlson L A. Six Degree of Freedom Dynamical Model of a Morphing Aircraft. *AIAA Atmospheric Flight Mechanics Conference*, Chicago, Illinois, AIAA Paper 2009-5849, 10-13 August 2009.
[10] Abdulrahim M and Lind R. Flight Testing and Response Characteristics of a Variable Gull-Wing Morphing Aircraft. *AIAA Guidance, Navigation, and Control Conference and Exhibit*, Providence, Rhode Island, AIAA Paper 2004- 5113, 16-19 August 2004.
[11] Abdulrahim M. Flight Performance Characteristics of a Biologically-Inspired Morphing Aircraft. *43rd AIAA Aerospace Sciences Meeting and Exhibit*, Reno, Nevada, AIAA Paper 2005-345, 10-13 January 2005.
[12] Abdulrahim M and Lind R. Using Avian Morphology to Enhance Aircraft Maneuverability. *AIAA Atmospheric Flight Mechanics Conference and Exhibit*, Keystone, Colorado, AIAA Paper 2006-6643, 21-24 August 2006.
[13] Grant D T., Chakravarthy A and Lind R. Modal Interpretation of Time- Varying Eigenvectors of Morphing Aircraft. *AIAA Atmospheric Flight Mechanics Conference*, Chicago, Illinois, AIAA Paper 2009-5848, 2009.
[14] Liu Y Z, Hong J Z and Yang H X. *Multibody system dynamics*. 1st edition, Advanced Education Press, 1989.

Copyright Statement